

Changes in microRNA and mRNA Expression with Differentiation of Human Bronchial Epithelial Cells

Asuncion Martinez-Anton¹, Milena Sokolowska¹, Steven Kern¹, A. Sally Davis², Sara Alsaaty¹, Jeffery K. Taubenberger², Junfeng Sun¹, Rongman Cai¹, Robert L. Danner¹, Michael Eberlein¹, Carolea Logun¹, and James H. Shelhamer¹

¹Critical Care Medicine Department, Clinical Center, and ²Viral Pathogenesis and Evolution Section, Laboratory of Infectious Disease, National Institute of Allergy and Infectious Disease, National Institutes of Health, Bethesda, Maryland

We studied the changes in expression of microRNAs (miRNAs or miRs) and mRNA in normal human bronchial epithelial cells as they differentiate from an undifferentiated monolayer to a differentiated pseudostratified epithelium after 28 days of air-liquid interface (ALI) culture. After 28 days in ALI, the epithelial cells differentially expressed basal, ciliated, and goblet cell markers. Using Affymetrix microarrays, 20 human miRNAs were found to be up-regulated, whereas 35 miRNAs were found to be down-regulated in differentiated cells compared with undifferentiated cells. An analysis of changes in global mRNA expression revealed that 1,201 probe sets demonstrated an 8-fold change (FC) or greater at Day 28 of ALI culture. Of these, 816 were up-regulated and 385 were down-regulated. With differentiation, miR-449a increased (FC, 38.15), and was related to changes in mRNA for cell division cycle 25 homolog A (FC, 0.11). MiR-455 decreased (FC, 0.12) and was related to changes in mRNA for the epithelial cell marker, mucin 1 (FC, 136). Transfection with anti-miR-449 or miR-455-3p resulted in changes in target protein expression (cell division cycle 25 homolog A and mucin 1, respectively), whereas transfection with reporter genes with 3'-untranslated regions of these targets confirmed control of expression through that structure. Therefore, changes in specific miRNAs during human airway epithelial cell differentiation control gene and protein expression important for differentiation.

Keywords: airways epithelium; differentiation; microarrays; mucin 1; cell division cycle homolog A

The human airway epithelium is a pseudostratified columnar epithelium containing basal, mucus-secreting (goblet), ciliated, and nonciliated cells. Under normal physiological conditions, the respiratory epithelium is covered by a mucus layer, the main role of which is to cover and protect the respiratory tract by trapping pathogens and irritant substances and to facilitate their removal by mucociliary clearance. In addition, the airway mucosa, through its epithelium, serves other functions, such as a physical barrier, transport, secretion, and modulation of inflammation (1). Defects in any of these functions are associated with a wide range of respiratory disorders, such as cystic fibrosis (2), asthma (3), and chronic obstructive pulmonary disease (4). For this reason, it is crucial to understand the molecular mechanisms regulating the mucociliary differentiation process and the role that it plays in mucosal function.

(Received in original form September 19, 2012 and in final form March 20, 2013)

This work was supported by the National Institutes of Health intramural research program.

Correspondence and requests for reprints should be addressed to James H. Shelhamer, M.D., National Institutes of Health, 9000 Rockville Pike, Building 10, Room 2C145, Bethesda, MD 20892. E-mail: jshelhamer@cc.nih.gov

This article has an online supplement, which is accessible from this issue's table of contents at www.atsjournals.org

Am J Respir Cell Mol Biol Vol 49, Iss. 3, pp 384–395, Sep 2013

Published 2013 by the American Thoracic Society

Originally Published in Press as DOI: 10.1165/rcmb.2012-0368OC on April 13, 2013

Internet address: www.atsjournals.org

CLINICAL RELEVANCE

The study presents data on changes in microRNA and mRNA as human bronchial epithelial cells differentiate.

Normal human bronchial epithelial (NHBE) cells cultured in an air-liquid interface (ALI) system form a polarized, pseudostratified epithelium composed of basal, ciliated, and goblet cells that closely resembles the *in vivo* airway epithelium (5). In addition to structural similarities, two recent publications have found a good correlation of global gene expression profiling between NHBE cells grown in an ALI and NHBE obtained from bronchial brushings (6, 7). Thus, ALI cultures of NHBE cells provide a unique *in vitro* system to investigate airway epithelial biology, including developmental, structural, and physiologic aspects. The ALI culture system has been used to study many aspects of epithelial biology, such as innate immune defense and injury and repair (8–14).

MicroRNAs (miRNAs or miRs) are short, single-stranded, noncoding RNAs of 20 to 23 nucleotides that down-regulate gene expression by either inducing degradation of target mRNAs or impairing their translation (15). They are phylogenetically well conserved, which implies an important role of miRNAs in biological processes. They are thought to regulate more than 30% of all protein-coding genes (16), and have been found to be involved in the regulation of development (17), proliferation (18), differentiation (19), apoptosis (20), and the immune response (21).

Several studies have dealt with the regulatory role of miRNA in the differentiation process of adipocytes (22), cardiac (23), neural (24), and hematopoietic (19) cell lineages. In addition, some miRNAs have been recently shown to regulate genes involved in epithelial cell differentiation. In this regard, miR-338-3p and miR-451 contribute to the formation of basolateral polarity in intestinal epithelial cells (25), and the miR-17 family controls FGF-10-mediated embryonic lung epithelial branching morphogenesis (26), whereas miR-7 modulates CD98 expression during intestinal epithelial cell differentiation (27). However, miRNA-specific roles and the relationship with their mRNA targets during airway epithelium differentiation are still not well defined.

The use of miRNA microarrays makes it possible to perform profiling studies that evaluate differences between healthy and pathologic tissues, treated and untreated samples, and undifferentiated and differentiated cells. Moreover, this systematic screening approach provides us with a starting point for the identification of new miRNA functions. In the present study, NHBE cells grown in an ALI culture system were globally screened using both miRNA and gene expression microarrays to identify miRNAs involved in the regulation of genes that are important for mucociliary differentiation in human airway epithelium.

MATERIALS AND METHODS

Cell Culture

Primary NHBE cells were obtained from Lonza (Walkersville, MD) and cultured in an ALI following the manufacturer's recommendations. Cells were harvested for total RNA extraction when they were sub-confluent or confluent, and after 14 or 28 days of ALI culture. A549 cells were obtained from ATCC (Manassas, VA) and cultured in Ham's F12 media with glutamine and 10% FCS (Invitrogen, Carlsbad, CA).

See the MATERIALS AND METHODS section in the online supplement for additional information on cells, microscopy, miRNA and gene arrays, real-time PCR, lentiviral transduction of NHBE cells, 3'-untranslated region (UTR) luciferase reporter assays, Western blot, and statistical analysis.

RESULTS

Morphology

To show the morphology and cellular composition of our NHBE undifferentiated and differentiated model, hematoxylin and eosin staining and immunofluorescence for specific cell markers were performed in confluent and Day-28 ALI cells. Undifferentiated confluent cells (Figures 1A–1D) and Day-28 ALI differentiated NHBE cells (Figures 1E–1H) were stained with a basal cell marker (anti-cytokeratin 5), a ciliated cell marker (anti- β -tubulin), and a goblet cell marker (Jacalin). Surprisingly, undifferentiated basal cells in monolayer apparently coexpressed all these markers at a certain level, partially colocalizing in the

cell cytoplasm (Figure 1D). Differentiated pseudostratified columnar epithelium after 28 days of ALI culture demonstrated differential expression for the mentioned markers within the columnar epithelial cells (Figures 1E–1H), indicating that the three main cell types that compose differentiated NHBE were present in our model. Hematoxylin and eosin staining showed similar cellular composition and distribution among the three donor samples (Figures 1I–1K). A differential interference contrast image shows cilia in the apical part of the differentiated epithelium, as well as secretory granules in mucous-secreting cells (Figure 1L).

Global miRNA Expression Profiling of Differentiating NHBE Cells

To identify miRNAs involved in the process of epithelial cell proliferation and differentiation, an miRNA expression profile analysis of cultured NHBE cells was performed using the Affymetrix GeneChip miRNA array (Santa Clara, CA). NHBE cells were cultured and harvested at three different time points: sub-confluent (cells dispersed on the insert under submerged conditions), confluent (cells forming a monolayer of undifferentiated cells covering the surface of the insert), and at Day 28 of ALI culture (cells were differentiated and had formed a polarized, pseudostratified mucociliary epithelium that resembles the *in vivo* airway epithelium structure).

To visualize the consistency between replicates and global changes within/between the studied groups, a principal components

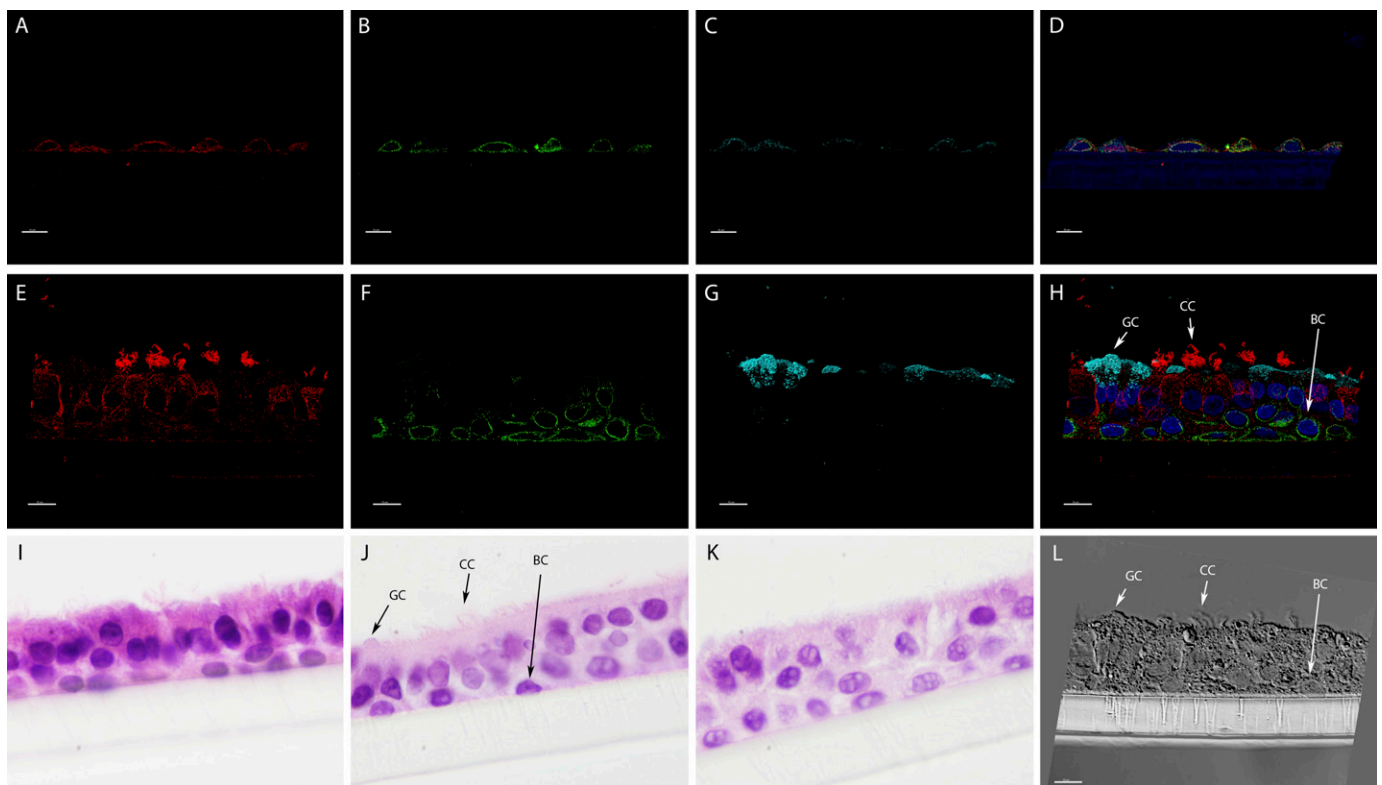


Figure 1. Confocal images of confluent and fully differentiated normal bronchial epithelial cells. Top row shows the confluent monolayer on its membrane labeled as follows: (A) ciliated cell (CC) marker, anti- β -tubulin (red); (B) basal cell (BC) marker, anti-cytokeratin 5 (green); (C) goblet cell (GC) marker, lectin jacalin (cyan); (D) fluorescence merge with above three markers along with DRAQ5 nuclear marker (blue). The central row (E–H) shows Day 28 air-liquid interface (ALI) fully differentiated, pseudostratified epithelium on its membrane labeled as above for the confluent monolayer. The bottom row includes (I–K) hematoxylin and eosin–stained sections of the differentiated pseudostratified epithelium on its membrane for each of the three donors studied (original magnification $\times 1,000$) and (L) a max projection of a differential interference contrast stack composed of a slice where the cilia are in focus and a slice with intracellular goblet cell mucins in focus imaged at the same physical slide location as in (E–H). All confocal images were taken at $630\times$ magnification at a zoom of $2.3\times$ and are maximum projections of z stacks unless otherwise noted. (scale bars, 10 μm).

analysis (PCA) of the Robust Multichip Analysis (RMA)-summarized probe sets was performed. This revealed a strong separation between all three groups, and good homogeneity within each group (Figure 2A). PCA of the data also showed that the primary determinant of differences was due to the differentiation state of the cells (i.e., undifferentiated [subconfluent and confluent] versus differentiated [Day-28 ALI] cells). Normalized data were further compared as described in the MATERIALS AND METHODS section, and differentially expressed miRNAs were selected by a false discovery rate less than 0.05 and 2-fold change (FC) for each comparison. A total of 74 and 55 human miRNAs were found differentially expressed between subconfluent and Day-28 ALI, and confluent and Day-28 ALI cells, respectively (Figure 2C). A total of 80% of the differentially expressed miRNAs in confluent compared with Day-28 ALI cells were also differentially expressed in subconfluent compared with Day-28 ALI cells. We did not find any miRNAs that were differentially expressed using these criteria between subconfluent and confluent cells. Therefore, for subsequent analyses, we focused on the differences between confluent (undifferentiated) and Day-28 ALI (differentiated) cells. The resulting miRNA list for this comparison is shown in Figure 3, together with the heat map showing the FCs in shades of *green* (decreased expression) and *red* (increased).

To understand the biological processes occurring during the differentiation of NHBE cells that might be regulated by our list of miRNAs, we performed a broad miRNA classification analysis using the *Tool for Annotations of MicroRNAs* (TAM) (28). Among miRNAs identified as up-regulated or down-regulated, there is a group involved in the regulation of cell cycle and cell proliferation (up: miR-200b, miR-200c, miR-449a, miR-449b, miR-34a, miR-34c, and miR-92b; down: miR-20a, miR-15b, miR-16, miR-125b, miR-17, miR-138, miR-27a, miR-18a, miR-205, miR-92a, miR-155, and miR-222). In the down-regulated group, we found two miRNA clusters highly represented: cluster 17–92 (miR-17, miR-18a, miR-20a, and miR-92a-1) and cluster 106a-363 (miR-106a, miR-20b, and miR-92a-2), primarily considered as oncomirs. Some of these clustered miRNAs, together with other down-regulated miRNAs, including miR-15b, miR-125b, miR-27a, miR-155, miR-30c, and miR-222, have been reported to be involved in human embryonic stem cell regulation.

Global Gene Expression Profiling of Differentiating NHBE Cells

To identify genes involved in epithelial cell proliferative and differentiation processes, a transcriptional analysis of cultured NHBE cells was performed using the Affymetrix Human Genome U133 Plus 2.0 array, which represents more than 47,000

transcripts. For gene expression profile analysis, the same time points (subconfluent, confluent, and Day-28 ALI cells) were analyzed using the RMA summarization algorithm. To visualize the consistency between replicates and global changes within/between the studied groups, a PCA of the RMA-summarized probe sets was performed, which revealed a strong separation between all three groups and good homogeneity within each group (Figure 2B). PCA of the data also showed that the primary determinant of differences was due to differentiation. Totals of 1,370 and 1,201 probe sets were found to be differentially expressed between subconfluent and Day-28 ALI, and confluent and Day-28 ALI cells, respectively. Only six probe sets were found to differ between subconfluent and confluent cells (Figure 2D). Therefore, for subsequent analysis, we focused on the differences between confluent (undifferentiated) and Day-28 ALI (differentiated) cells. From the 1,201 probe sets showing differences between confluent and Day-28 ALI cells, 816 were up-regulated and 385 down-regulated in Day-28 ALI cells compared with confluent cells. The number of genes that had a known function or cellular localization and thus could be annotated were 607 and 260, found to be up-regulated and down-regulated, respectively, in Day-28 ALI cells compared with confluent cells.

To understand the biological processes occurring during differentiation of NHBE cells, we performed a broad gene classification analysis. Classified genes presenting the highest changes are listed in Tables 1–3 and Tables E1–E7 in the online supplement, and include genes encoding for cytokines and secreted proteins (Table 1 and Table E1), cell surface and membrane-bound proteins (Table 1 and Table E2), cytoskeleton proteins (Table 2 and Table E3), signal transduction proteins (Table 2 and Table E4), transcriptional regulation and nucleotide-binding proteins (Table 2 and Table E5), cell cycle and apoptotic proteins (Table 3 and Table E6), and metabolic pathway proteins (Table 3 and Table E7).

During the differentiation process of NHBE cells, 38 genes coding for cytokines and secreted proteins and 124 genes coding for cell surface and membrane-bound proteins were found increased in differentiated compared with undifferentiated cells (Table 1 and Table E1). These include secretoglobin family members (SCGB1A1, -2A1, -3A1), chemokine ligands (CXCL6, -17, CX3CL1), and IL-19. Mucins (mucin [MUC] 1, MUC4, MUC15, MUC20), major histocompatibility complex molecules (HLA-DRA, -DQA1, -DPA1, -DRB1), and solute carrier family members (SCL6A14, -46A3, -15A2) were among the membrane-bound category. Cytoskeleton proteins induced by differentiation included several members of the dynein, tubulin, and keratin families (Table 2 and Table E3). A total of 59 genes involved in signal

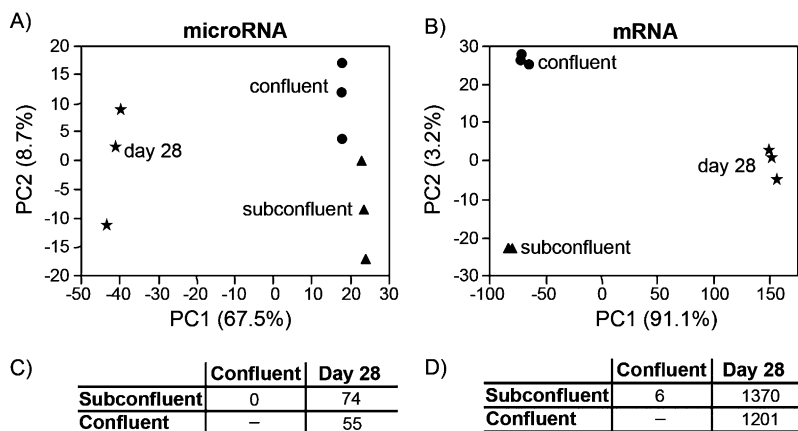
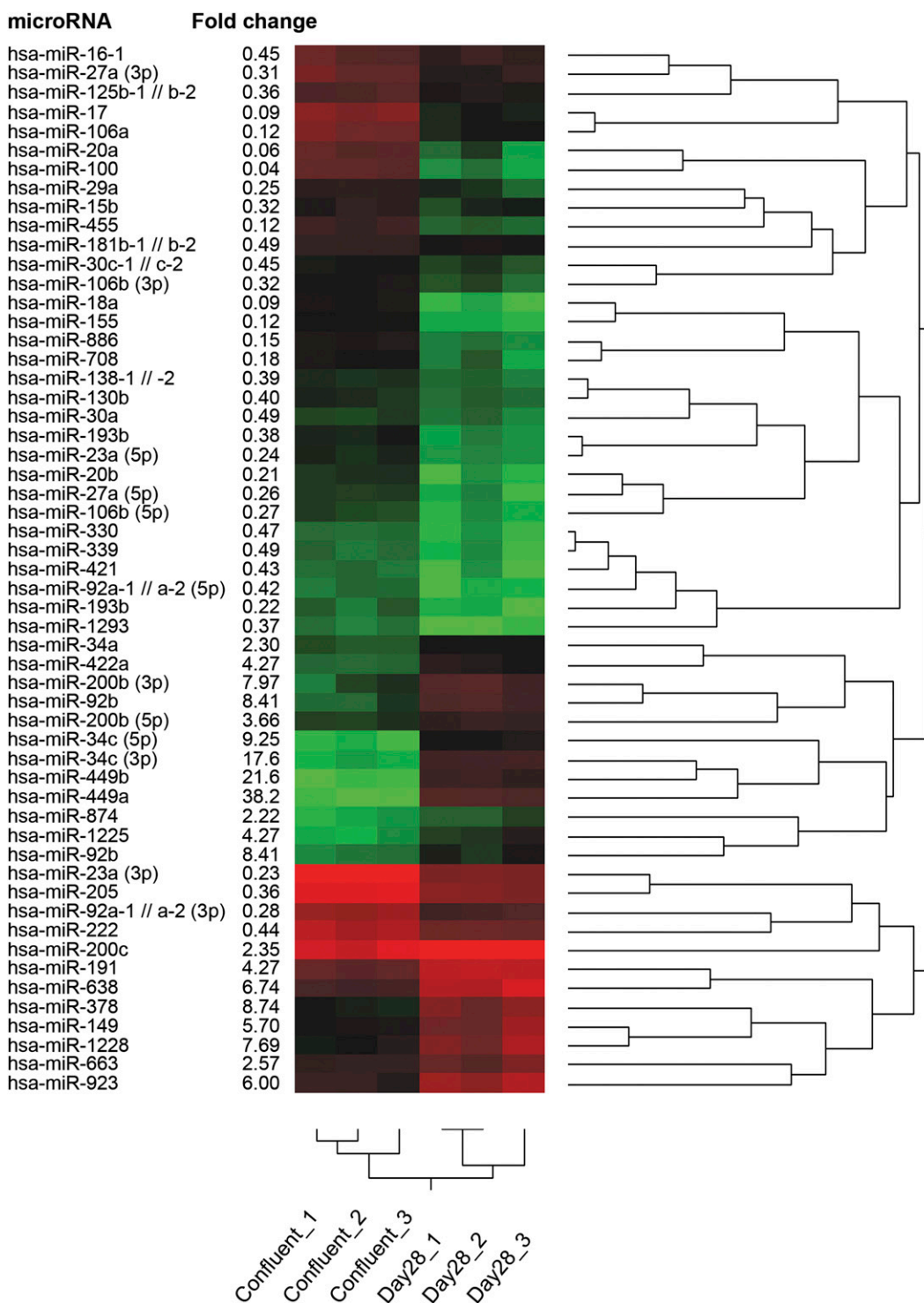


Figure 2. Principal components analysis (PCA) of microRNA (miRNA or miR) (A) and mRNA (B) normalized expression data from differentiating normal human bronchial epithelial cells. The PCA of the data revealed strong separation between all the groups and good homogeneity within each group, for both miRNA and gene arrays. Expression data from three independent cultures from a single donor indicate that the predominant difference among the culture conditions is the difference between differentiated cells at Day 28 (star) and subconfluent (triangle) and confluent (circle) cells. (C and D) Summary of the number of probe sets that displayed a 2-fold change (miRs) and 8-fold change (mRNA) (increase or decrease) between the different groups: subconfluent; confluent; Day-28 normal human bronchial epithelial (NHBE) cells grown in an ALI culture system for 28 days.



transduction were increased in differentiated compared with undifferentiated cells, including several members of G protein-coupled receptors (GPR98, -C5B, -160) and signaling kinases (MAP3K8, STK33, CAMK1B, ERBB4) (Table 2 and Table E4). Tables 2–3 and Tables E5–E6 present the effect of differentiation on genes involved in transcriptional regulation (ELF3, SMAD9, MYB, SOX2), cell cycle, and apoptosis (cell division cycle [CDC] homolog 20B, DAPL1, CCNA1, CDKN28). Finally, differentiation induced the expression of 116 genes that have roles in cellular metabolism (Table 3 and Table E7). These include genes involved in redox (ALDH1A1, ADH7, CYP2B6, -7P1)

and carbohydrate (MDH1B, PDK4, CHST9, GCNT3) metabolism, as well as many others. By contrast, the list of genes found to be down-regulated in differentiated compared with undifferentiated cells was shorter. Only 24 genes coding for cytokines and secreted proteins, such as IL-1 α and IL-1 β , collagen molecules, and laminins, were part of the list of down-regulated genes (Table 1 and Table E1). Cytoskeleton family members, such as vimentins and kinesins, were also found down-regulated in differentiated compared with undifferentiated cells (Table 2 and Table E3). Finally, signal transduction (DUSP6, DUSP7) as well as cell cycle and apoptosis (CDC6, CDC7, CDC25A,

TABLE 1. GENES PRESENTING CHANGES IN DIFFERENTIATED (DAY28) COMPARED TO UNDIFFERENTIATED CELLS (CONFLUENT)

Entrez ID	Name	Symbol	Fold Change
Cytokines and secreted proteins (38 up; 24 down)			
155,465	Anterior gradient homolog 3	AGR3	1,016.45
6,779	Statherin	STATH	807.65
92,304	secretoglobin, family 3A, member 1	SCGB3A1	554.89
6,947	Transcobalamin I	TCN1	488.85
12	Serpin peptidase inhibitor, clade A, member 3	SERPINA3	272.41
629	Complement component 2/complement factor B	C2/CFB	227.69
7,356	Secretoglobin, family 1A, member 1	SCGB1A1	149.85
4,246	Secretoglobin, family 2A, member 1	SCGB2A1	129.96
3,553	Interleukin-1 β	IL1B	0.03
3,956	Lectin, galactoside-binding, soluble, 1	LGALS1	0.03
5,270	Serpin peptidase inhibitor, clade E, member 2	SERPINE2	0.02
4,312	Matrix metalloproteinase 1	MMP1	0.02
3,552	Interleukin-1 α	IL1A	0.01
Cell surface and membrane-bound proteins (124 up; 52 down)			
4,477	Microseminoprotein, β	MSMB	1,297.43
51,297	Palate, lung and nasal epithelium associated	PLUNC	1,088.5
132,203	Sentan, cilia apical structure protein	SNTN	693.51
4,974	Oligodendrocyte myelin glycoprotein	OMG	591.53
3,122	Major histocompatibility complex, class II, DR α	HLA-DRA	457.83
8,842	Prominin 1	PROM1	269.67
1,356	Ceruloplasmin	CP	235.67
2,568	γ -aminobutyric acid A receptor, pi	GABRP	229.23
79,838	Transmembrane channel-like 5	TMC5	207.06
94,122	Synaptotagmin-like 5	SYTL5	196.88
148,808	Major facilitator superfamily domain containing 4	MFSD4	177.54
4,585	Mucin 4	MUC4	146.23
4,582	Mucin 1	MUC1	136.21
79,679	V-set domain containing T cell activation inhibitor 1	VTCN1	127.38
9,073	Claudin 8	CLDN8	117.10
143,662	Mucin 15, cell surface associated	MUC15	100.42
8,000	Prostate stem cell antigen	PSCA	89.97
200,958	Mucin 20, cell surface associated	MUC20	82.53
3,117	Major histocompatibility complex, class II, DQ α 1	HLA-DQA1	80.42
284,013	Vitellogenesis membrane outer layer 1 homolog	VMO1	63.60
10,537	γ -aminobutyric acid (GABA) B receptor, 1/ubiquitin D	GABBR1/ UBD	62.32
100,294,224	Major histocompatibility complex, class II, DQ α 1/ 2	HLA-DQA1/ A2	60.64
94,025	Mucin 16, cell surface associated	MUC16	60.29
64,446	Dynein, axonemal, intermediate chain 2	DNAI2	59.29
3,909	Laminin, α 3	LAMA3	0.05
22,943	Dickkopf homolog 1	DKK1	0.05
5,010	Claudin 11	CLDN11	0.04
51,309	Armadillo repeat containing, X-linked 1	ARMCX1	0.04
8,140	Solute carrier family 7, member 5	SLC7A5	0.04
2,069	Eprexulin	EREG	0.04
4,162	Melanoma cell adhesion molecule	MCAM	0.03
10,544	Protein C receptor, endothelial	PROCR	0.03
1,009	Cadherin 11, type 2, OB-cadherin	CDH11	0.02
9,638	Fasciculation and elongation protein zeta 1	FEZ1	0.02
8,406	Sushi-repeat-containing protein, X-linked	SRPX	0.02
347,902	Adhesion molecule with Ig-like domain 2	AMIGO2	0.01

Definition of abbreviation: OB, osteoblast.

CCDNA2, CCDND2, CHEK1) regulatory genes were also diminished in the differentiated cells (Tables 2–3 and Tables E4–E6). A list of 192 genes of unclassified function is also included in the online supplement (Table E8).

In addition, we performed an unsupervised hierarchical clustering of the genes differentially expressed between undifferentiated and differentiated NHBE cells, and selected four main clusters, which represented groups of genes showing similar changes. Two of them presented genes up-regulated in differentiated compared with undifferentiated cells, and the other two consisted of genes down-regulated in differentiated cells. The four-cluster gene lists were interrogated for enrichment of known biological labels using the functional annotation clustering analysis by DAVID (<http://david.abcc.ncifcrf.gov>). The heat maps and the list of biological categories found enriched in the four main clusters selected are

shown in Figure E1. Briefly: cluster A was primarily enriched in cilium biogenesis and degradation terms, as well as in extracellular matrix components; cluster B was enriched in categories related to extracellular region/signaling components, immune response, and oxidation/reduction processes; cluster C was enriched in mitotic cell cycle, spindle organization and localization, and cytoskeleton-related categories; cluster D was enriched in microtubule cytoskeleton, cell cycle, extracellular region/signaling, and DNA replication terms. The complete list of genes comprising these four clusters is presented in Table E9.

Confirmatory Experiments

To verify and validate data obtained from microarray studies, two additional techniques were used: real-time PCR (mRNA

TABLE 2. GENES PRESENTING CHANGES IN DIFFERENTIATED (DAY28) COMPARED TO UNDIFFERENTIATED CELLS (CONFLUENT)

Entrez ID	Name	Symbol	Fold Change
Cytoskeleton proteins (39 up; 23 down)			
83,657	Dynein, light chain, roadblock-type 2	DYNLRB2	255.01
5,304	Prolactin-induced protein	PIP	185.46
9,576	Sperm associated antigen 6	SPAG6	183.52
10,568	Solute carrier family 34, member 2	SLC34A2	132.94
51,673	Tubulin polymerization-promoting protein family member 3	TPPP3	88.27
7,802	Dynein, axonemal, light intermediate chain 1	DNALI1	84.30
221,421	Radial spoke head 9 homolog	RSPH9	73.99
28,234	Solute carrier organic anion transporter family, member 1B3	SLCO1B3	70.64
9,055	Protein regulator of cytokinesis 1	PRC1	0.07
9,928	Kinesin family member 14	KIF14	0.06
800	Caldesmon 1	CALD1	0.06
81,624	Diaphanous homolog 3	DIAPH3	0.06
7,431	Vimentin	VIM	0.05
6,624	Fascin homolog 1, actin-binding protein	FSCN1	0.05
Signal transduction proteins (59 up; 23 down)			
133,690	Calcyphosine-like	CAPSL	377.28
158,798	A kinase anchor protein 14	AKAP14	351.61
5,918	Retinoic acid receptor responder 1	RARRES1	265.90
83,853	Ropporin 1-like	ROPN1L	184.74
58,528	Ras-related GTP binding D	RRAGD	132.70
479	ATPase, H ⁺ /K ⁺ transporting, nongastric, α polypeptide	ATP12A	132.39
151,651	EF-hand domain family, member B	EFHB	112.91
128,153	Spermatogenesis associated 17	SPATA17	92.40
57,460	Protein phosphatase 1H	PPM1H	73.98
828	Calcyphosine	CAPS	68.21
122,481	Adenylate kinase 7	AK7	65.49
64,798	DEP domain containing 6	DEPDC6	60.38
80,258	EF-hand domain containing 2	EFHC2	56.78
2,869	G protein-coupled receptor kinase 5	GRK5	0.05
9,590	A kinase anchor protein 12	AKAP12	0.05
5,880	ras-related C3 botulinum toxin substrate 2	RAC2	0.05
55,789	DEP domain containing 1B	DEPDC1B	0.05
558	AXL receptor tyrosine kinase	AXL	0.04
79,801	SHC SH2-domain binding protein 1	SHCBP1	0.03
Transcriptional regulation and nucleotide-binding proteins (41 up; 31 down)			
5,284	Polymeric immunoglobulin receptor	PIGR	1588.15
27,324	TOX high mobility group box family member 3	TOX3	165.93
5,450	POU class 2 associating factor 1	POU2AF1	52.92
6,035	RNase, RNase A family, 1	RNASE1	47.30
10,891	Peroxisome proliferator-activated receptor γ , coactivator 1 α	PPARGC1A	43.22
1,999	E74-like factor 3	ELF3	41.83
4,306	Nuclear receptor subfamily 3, group C, member 2	NR3C2	39.64
4,093	SMAD family member 9	SMAD9	36.15
161,582	Dyslexia susceptibility 1 candidate 1	DYX1C1	27.44
8,061	FOS-like antigen 1	FOSL1	0.05
4,603	v-myb myeloblastosis viral oncogene homolog like 1	MYBL1	0.05
89,795	Neuron navigator 3	NAV3	0.05
4,907	5'-nucleotidase, ecto	NT5E	0.04
79,413	Zinc finger, BED-type containing 2	ZBED2	0.02
10,468	Follistatin	FST	0.02

and miRNA expression) and Western blot analysis (protein expression). Real-time PCR quantification was performed for four miRNAs and five genes found to be up-regulated or down-regulated during the differentiation progress of NHBE cells. Hsa-miR-23a, hsa-miR-449a, hsa-miR-455-3p, and hsa-miR-125b were selected for validation by real-time PCR (Table 4). In addition, the following gene products were also selected for real-time validation: CDC25A, mucin 1 (MUC1), peroxisome proliferator-activated receptor γ coactivator α (PPARGC1A), IL-1 β , and IL6 (Table 4). CDC25A and MUC1 were also validated by Western blot (Figures 4C and 4D). Changes in mRNA and miRNA by real-time PCR and protein expression by Western blot appear to be consistent with the detected changes in mRNA and miRNA expression by microarray.

Prediction of miR-449a and miR-455-3p Targets

Several miRNAs found to be differentially expressed in differentiated cells (Day-28 ALI) compared with undifferentiated cells (confluent) were selected for further analysis to identify potential targets for these miRNAs focusing on the genes directly involved in proliferation or differentiation. Genes considered as differentiation markers for being exclusively expressed in differentiated ciliated or mucus-secreting cells were also taken into consideration. On the up-regulated miRNA list, miR-449a has been reported as a regulator of CDC25A in different biological models. CDC25A, a protein phosphatase involved in cell cycle progression (from G1 to the S phase), was greatly decreased (FC, 0.05) in our differentiated cells. Moreover, MUC1, a mucin that, in physiologic conditions, is involved in the protection of the

TABLE 3. GENES PRESENTING CHANGES IN DIFFERENTIATED (DAY28) COMPARED TO UNDIFFERENTIATED CELLS (CONFLUENT)

Entrez ID	Name	Symbol	Fold Change
Cell Cycle, Development and Apoptosis			
Proteins (18 up; 55 down)			
166,979	Cell division cycle 20 homolog B	CDC20B	555.08
89,765	Radial spoke head 1 homolog	RSPH1	293.43
58,480	Ras homolog gene family, member U	RHOU	96.09
92,196	Death associated protein-like 1	DAPL1	67.44
3,400	Inhibitor of DNA binding 4	ID4	31.84
9,837	GIN5 complex subunit 1	GIN51	0.06
6,241	Ribonucleotide reductase M2	RRM2	0.06
993	Cell division cycle 25 homolog A	CDC25A	0.05
55,165	Centrosomal protein 55 kD	CEP55	0.05
1,111	CHK1 checkpoint homolog	CHEK1	0.05
51,659	GIN5 complex subunit 2	GIN52	0.05
22,822	Pleckstrin homology-like domain, family A, member 1	PHLDA1	0.05
51,514	Denticleless homolog	DTL	0.05
57,405	SPC25, NDC80 kinetochore complex component, homolog	SPC25	0.04
50,486	G0/G1 switch 2	G0S2	0.04
83,879	Cell division cycle associated 7	CDCA7	0.04
990	Cell division cycle 6 homolog	CDC6	0.04
29,775	Caspase recruitment domain family, member 10	CARD10	0.03
Metabolism proteins (116 up; 32 down)			
1,580	Cytochrome P450, family 4, subfamily B, polypeptide 1	CYP4B1	761.35
2,938	Glutathione S-transferase α 1	GSTA1	285.28
8,424	Butyrobetaine, 2-oxoglutarate dioxygenase 1	BBOX1	208.5
126	Alcohol dehydrogenase 1C, γ polypeptide	ADH1C	199.83
92,291	Calpain 13	CAPN13	173.79
79,740	Zinc finger, B-box domain containing	ZBBX	165.87
10,406	WAP four-disulfide core domain 2	WFDC2	123.76
1,555	Cytochrome P450, family 2, subfamily B, polypeptide 6	CYP2B6	122.73
8,418	Cytidine monophosphate-N-acetylneuraminic acid hydroxylase	CMAH	114.47
216	Aldehyde dehydrogenase 1 family, member A1	ALDH1A1	111.65
6,317	Serpin peptidase inhibitor, clade B, member 3	SERPINF3	111.56
1,556	Cytochrome P450, family 2, subfamily B, polypeptide 7 pseudogene 1	CYP2B7P1	77.17
130,752	Malate dehydrogenase 1B, NAD	MDH1B	71.12
5,166	Pyruvate dehydrogenase kinase, isozyme 4	PKD4	70.83
4,069	Lysozyme	LYZ	70.69
23,120	ATPase, class V, type 10B	ATP10B	69.62
240	Arachidonate 5-lipoxygenase	ALOX5	58.78
1,733	Deiodinase, iodothyronine, type I	DIO1	57.85
154,865	IQ motif and ubiquitin domain containing	IQUB	57.11
9,245	Glucosaminyl (N-acetyl) transferase 3, mucin type	GCNT3	55.31
131	Alcohol dehydrogenase 7, μ or σ polypeptide	ADH7	53.28
26,960	Neurobeachin	NBEA	52.06
3,992	Fatty acid desaturase 1	FADS1	0.07
29,128	Ubiquitin-like with PHD and ring finger domains 1	UHRF1	0.06
7,298	Thymidylate synthetase	TYMS	0.06
8,877	Sphingosine kinase 1	SPHK1	0.06
4,017	Lysyl oxidase-like 2	LOXL2	0.04
7,378	Uridine phosphorylase 1	UPP1	0.04
26,278	Spastic ataxia of Charlevoix-Saguenay	SACS	0.03
9,388	Lipase, endothelial	LIPG	0.02

Definition of abbreviation: NAD, nicotinamide adenine dinucleotide.

airways from pathogens, was increased (FC, 136.2) in the differentiated epithelium, and found to be a potential target for miR-455-3p, which was significantly down-regulated (FC, 0.12) in differentiated cells. As noted, those expression changes found by microarray for CDC25A, MUC1, miR-449a, and miR-455-3p in our epithelial differentiation model were confirmed by real-time PCR and Western blot (CDC25A and MUC1) (Table 4 and Figure 4). Moreover, the observed reciprocal changes in miRNAs and their putative targets suggested a possible causal relationship.

Anti-miR-449a Increases CDC25A Expression in NHBE Cells

Expression of miR-449a increases, whereas CDC25A expression decreases, during the differentiation process of NHBE cells

(from confluent to Day 28 of ALI culture). To examine whether miR-449a regulates CDC25A expression, a loss-of-function analysis for miR-449a was performed during the differentiation of NHBE cells. NHBE cells were transduced with lentiviral particles containing a scrambled anti-miRNA (anti-miR control) or an anti-miR-449a scaffold. After 14 days of ALI culture, CDC25A expression levels were assessed by real-time RT-PCR and Western blot. Due to the limited expression of CDC25A at Day 28 of ALI culture, the analysis was performed at Day 14. Cells not transduced were used as a negative control for transduction effects *per se* and/or anti-miR control effects. The green fluorescent protein (GFP) reporter gene inserted together with anti-miR-449a precursor in the expression vector appeared to be transduced in 60% of NHBE cells (data not shown). In addition, miR-449a expression was determined by real-time

TABLE 4. COMPARISON OF RT-PCR AND MICROARRAY RESULTS

			Day 28/C Fold Change (95% CI)*	
Identification			RT-PCR	Array
microRNA	microRNA ID	MIMAT		
microRNA sequence				
AUCACAUUGCCAGGGAUUUCC	hsa-miR-23a	0000078	0.60 (0.56–0.64)	0.23 (0.19–0.3)
UGGCAGUGUAUUGUAGCUGGU	hsa-miR-449a	0001541	7,171.29 (5,430.51–9,470.07)	38.15 (29.33–49.6)
GCAGUCCAUGGGCAUAUACAC	hsa-miR-455-3p	0004784	0.09 (0.08–0.10)	0.12 (0.1–0.14)
UCCUGAGACCCUAACUUGUGA	hsa-miR-125b-1//2	0000423	0.36 (0.34–0.39)	0.36 (0.26–0.48)
mRNA	Gene Symbol	Entrez Gene		
Gene name				
Cell division cycle 25 homolog A	CDC25A	993	0.17 (0.12–0.24)	0.05 (0.03–0.07)
Mucin 1	MUC1	4,582	893.09 (674.54–1,182.44)	136.21 (117.62–157.73)
Peroxisome proliferator-activated receptor γ , coactivator α	PPARGC1A	10,891	202.14 (164.67–248.14)	43.22 (36.42–51.29)
Interleukin-1 β	IL1B	3,553	0.06 (0.03–0.10)	0.03 (0.02–0.03)
Interleukin-6	IL6	3,569	0.29 (0.10–0.80)	0.4 (0.37–0.43)

Definition of abbreviations: C, confluent; CI, confidence interval; hsa, homo sapiens; MIMAT, mature microRNA accession number; miR, microRNA.

*Fold change of normal human bronchial epithelial cells grown in an air-liquid interface for 28 days over undifferentiated confluent cells. RT-PCR data represent fold change means from three different donors. Array data represent fold change means from three independent cultures from a single donor.

RT-PCR, showing that the transduced anti-miR-449a was efficiently decreasing miR-449a expression (FC, 0.25) in NHBE cells at 14 days of ALI culture compared with negative control cells (Figure 5A). We assessed the effects of miR-449a down-regulation on CDC25A expression levels. Anti-miR-449a was found to increase CDC25A mRNA levels (FC, 1.86) at Day 14 of ALI in transduced NHBE cells compared with negative control cells, but this increase was not statistically significant (Figure 5B). By Western blot analysis, CDC25A protein levels were increased upon transduction of anti-miR-449a at Day 14 of ALI culture (Figure 5C). Therefore, miR-449a appears to regulate CDC25A expression at the translational level.

Hsa-miR-449a Directly Targets the 3'-UTR of CDC25A

The CDC25A 3'-UTR contains one miR-449a-binding site, as suggested by TargetScan. Because differentiated NHBE cells are difficult to transfect with plasmids, we used the human lung epithelial cell line, A549 cells, to study the role of miR-449a in the expression of CDC25A. To determine if miR-449a suppresses CDC25A expression by directly binding to CDC25A 3'-UTR,

a reporter luciferase vector containing the full-length CDC25A 3'-UTR sequence was transfected into A549 cells in the presence or absence of miR-449a. As shown in Figure 5D, miR-449a significantly decreased the luciferase activity by roughly 50% after 48 hours of transfection in A549 cells, indicating that miR-449a targets and down-regulates CDC25A expression by directly interacting with its 3'-UTR. In contrast, the miR control slightly increased luciferase activity compared with the untransfected control.

Hsa-miR-455-3p Inhibits MUC1 Expression in NHBE Cells

MiR-455-3p expression decreases, whereas MUC1 expression increases, during the differentiation process of NHBE cells. To examine the regulation exerted by miR-455-3p on MUC1 expression, a gain-of-function analysis for miR-455-3p was performed during the differentiation of NHBE cells. NHBE cells were transduced for 14 days with lentiviral particles containing scrambled miRNA (miR control) or the mature miR-455-3p scaffold, and MUC1 expression levels were assessed by real-time RT-PCR and Western blot. The GFP reporter gene inserted

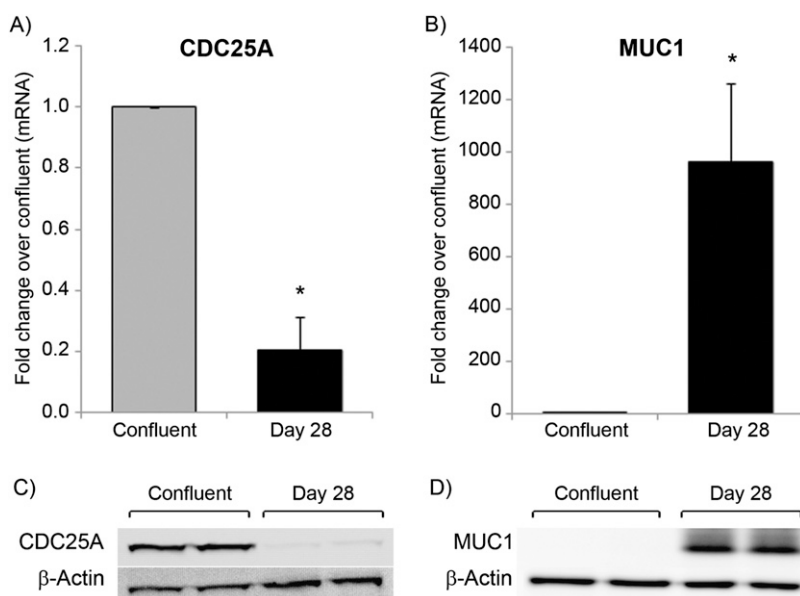


Figure 4. Cell division cycle (CDC) homolog 25A and mucin (MUC) 1 gene (A and B) and protein (C and D) expression in undifferentiated (confluent) and differentiated (Day 28) NHBE cells. Bar graphs indicate fold changes in expression of CDC25A (A) and MUC1 (B) mRNA relative to confluent cells. Results are expressed as mean \pm SEM (Student's *t* test: $*P < 0.05$) from three different donors. Western blot analysis of CDC25A (C) and MUC1 (D) protein levels in undifferentiated (confluent) and differentiated (Day 28) NHBE cells. The Western blot is representative of data from two separate experiments. β -actin expression is shown as a loading control.

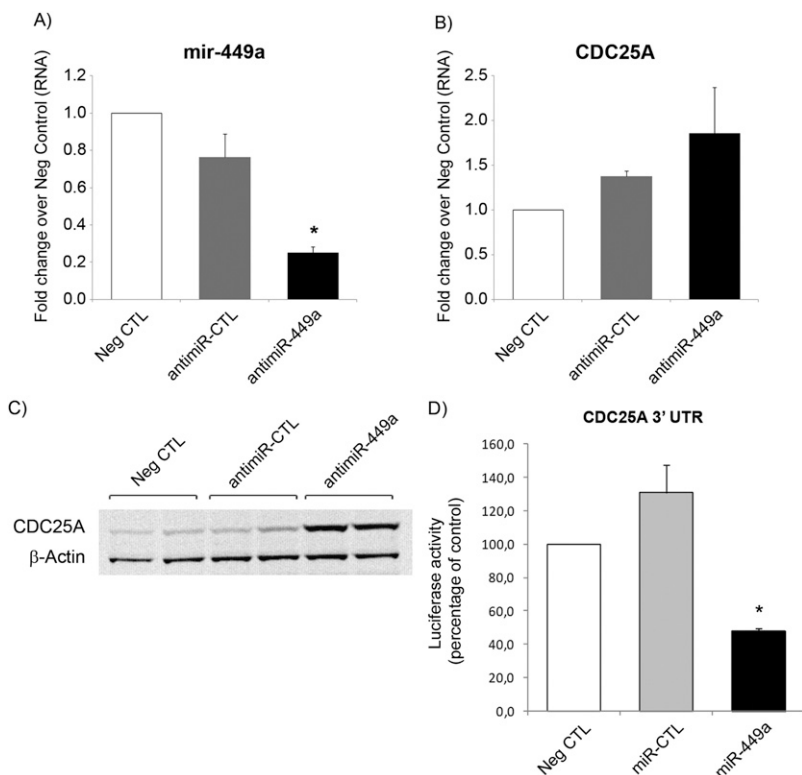


Figure 5. Effect of functional inhibition of miR-449a on CDC25A expression. NHBE cells were transduced when subconfluent with lentiviral particles expressing an anti-miR control or anti-miR-449a. Cells were harvested after 14 days of ALI culture. Bar graphs indicate fold changes in expression of miR-449a (A) and CDC25A (B) after anti-miR-449a transduction relative to negative control cells. Results from three independent cultures from a single donor are expressed as means \pm SEM (Student's *t* test: **P* < 0.05). (C) Western blot analysis of CDC25A protein levels after anti-miR-449a transduction compared with nontransduced (negative control) and anti-miR control-transduced cells. The Western blot is representative of data from two independent experiments. β -actin expression is shown as a loading control. (D) A549 cells were transfected with the CDC25A 3'-untranslated region (UTR)-luciferase construct in the presence or absence of 20 nM of miR control or miR-449a precursor. Luciferase activity was measured at 48 hours post-transfection. Results are expressed as means \pm SEM of three independent experiments, each assayed in triplicate (Student's *t* test: **P* < 0.05, compared with negative control cells).

together with the miR-455-3p precursor in the expression vector appeared to be transduced in over 90% of the cells (data not shown). In addition, miR-455-3p expression was determined by real-time RT-PCR, showing that miR-455-3p was efficiently expressed after lentiviral transduction in NHBE cells after 14 days (FC, 411.6) of ALI culture compared with negative control cells (Figure 6A). We then assessed the effects of miR-455-3p overexpression on MUC1 expression levels. MiR-455-3p was found to significantly decrease MUC1 mRNA levels in NHBE cells after 14 days of ALI culture (FC, 0.45) compared with negative control cells. The transduced miR control seemed to cause a nonspecific decrease in MUC1 mRNA (FC, 0.75). Nonetheless, miR-455-3p transduction resulted in a significant decrease in MUC1 mRNA levels compared with both negative control and miR control groups (Figure 6B). By Western blot analysis, MUC1 protein levels were found decreased upon transduction of miR-455-3p after 14 days of ALI culture (Figure 6C).

Hsa-miR-455-3p Directly Targets the 3'-UTR of MUC1

The MUC1 3'-UTR contains one miR-455-3p-binding site, as suggested by TargetScan. To determine if miR-455-3p suppresses MUC1 expression by directly binding to MUC1 3'-UTR, a reporter dual-luciferase vector containing the full-length MUC1 3'-UTR sequence was transfected into A549 cells in the presence or absence of miR-455-3p. As shown in Figure 6D, miR-455-3p significantly decreased luciferase activity by approximately 30% after 48 hours of transfection in A549 cells, indicating that miR-455-3p targets and down-regulates MUC1 expression by directly binding to its 3'-UTR. In contrast, the miR-control had no effect on luciferase activity in cells transfected with the MUC1 3'-UTR (Figure 6D).

In summary, in NHBE cells: (1) subsets of miRNAs (55) and genes (>1,000) are differentially expressed between differentiated and undifferentiated cells; (2) miR-449a (increased in

differentiated cells) targeted CDC25A, a gene involved in cell cycle progression; (3) miR-455-3p (decreased in differentiated cells) targeted MUC1, a marker of differentiated cells. In support of these conclusions we have demonstrated: (1) that anti-miR-449a increased CDC25A protein expression at Day 14 of ALI culture; and (2) that miR-455-3p decreased MUC1 gene and protein expression at Day 14 of ALI culture. In A549 cells, we have determined that miR-449a and miR-455-3p exerted their regulation on CDC25A and MUC1, respectively, by directly interacting with their 3'-UTR.

DISCUSSION

ALI cultures from human bronchial epithelial cells have been widely used to study human airway epithelium, from different physiologic and pathologic aspects. Recently, Dvorak and co-workers (6) demonstrated that ALI cultures of human bronchial epithelial cells represent the transcriptome of the airway epithelium *in vivo*. They showed that there was a large and significant overlap between the transcriptomes of human airway epithelium cultured *in vitro* in ALI and brushed cells obtained directly from airway epithelium from healthy individuals, with at least 81% of expressed genes showing similar expression profiles in both systems. In the present study, we used ALI cultures of NHBE cells as a model of airway epithelial differentiation. Using this cell culture approach, we have characterized global miRNA and gene expression profiles during differentiation of NHBE cells. In addition, using computational tools, we correlated selected miRNAs presenting changes during the differentiation process of NHBE cells with their potential targets, and performed gain- and loss-of-function studies to clarify the regulation exerted by these miRNAs on genes related to proliferative and/or differentiation processes of NHBE cells.

To our knowledge, this is the first time that a comprehensive miRNA array approach has been used to study the miRNA expression profile during human bronchial epithelial differentiation. In

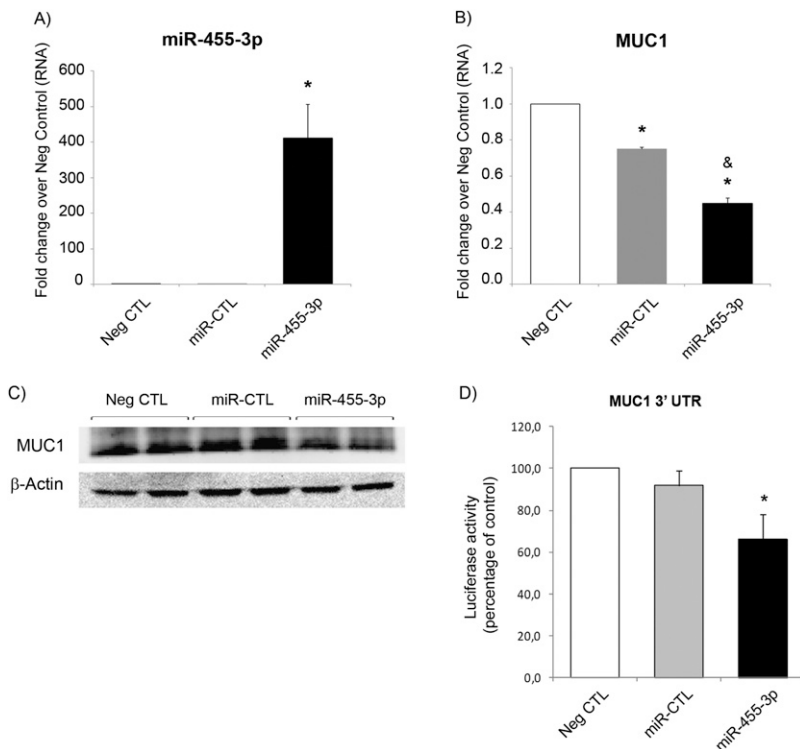


Figure 6. Effect of functional overexpression of miR-455-3p on MUC1 expression. NHBE cells were transduced when subconfluent with lentiviral particles expressing miR control or miR-455-3p, and harvested after 14 days of ALI culture. (A) Bar graphs indicate fold changes in expression of miR-455-3p (A) and MUC1 (B) after miR-455-3p transduction relative to negative control cells. Results from three independent cultures from a single donor are expressed as means \pm SEM (Student's *t* test: **P* < 0.05 compared with negative control [Neg CTL]; &*P* < 0.05 compared with miR-CTL). (C) Western blot analysis of MUC1 protein levels after miR-455-3p transduction compared with nontransduced (negative control) and miR control-transduced cells. The Western blot is representative of data from two independent experiments. β -actin expression is shown as a loading control. (D) A549 cells were transfected with the MUC1 3'-UTR-luciferase construct in the presence or absence of 20 nM of miR control or miR-455-3p precursor. Luciferase activity was measured at 48 hours post-transfection and normalized to the internal *Renilla* luciferase control. Results are expressed as means \pm SEM of three independent experiments, each assayed in triplicate (Student's *t* test: **P* < 0.05, compared with negative control cells).

this sense, these data provide an important molecular starting point for the study of the epithelial differentiation processes, and represent a useful resource for researchers interested in the regulation of proliferation, differentiation, and development of the respiratory epithelium.

In the present study, the most profound changes in both miRNA and gene expression profiles were found between undifferentiated (subconfluent and confluent groups) and differentiated cells (Day 28 of ALI culture), instead of between proliferating (subconfluent) and less-proliferating cells (confluent). This finding is not surprising, given that subconfluent and confluent cells consist of a homogeneous monolayer of epithelial cells, whereas differentiated cells at Day 28 of ALI consist of a mixed population of basal, ciliated, and mucus-secreting cells.

Some of the changes observed in our study might be due to the culture conditions used for the two different time-points studied—undifferentiated (confluent) and differentiated (Day-28 ALI) cells. Media composition (i.e., retinoic acid and epidermal growth factor at different concentrations), time in culture, and exposure to the air are key factors for the differentiation of primary epithelial cells into a polarized, pseudostratified epithelium containing basal, ciliated, and mucus-secreting cells. Any of these factors might be direct contributors to some of the changes in miRNA and gene expression differences reported here.

We identified a number of miRNAs that display significant increases (20 miRNAs) or decreases (35 miRNAs) during differentiation of NHBE cells. Many of them have established functions in cell cycle progression, either inducing proliferation or growth arrest. MiR-34 and miR-449 family members were found to be highly increased in differentiated cells in our model, and have been reported to be induced in the differentiation processes in other models, such as human nasal epithelial cells, *Xenopus laevis* embryonic epidermis (29), and mouse neural stem cells (30). A recent study also showed that miR-449a and miR-34c were among the 45 most highly expressed miRNAs in differentiated human airway epithelial cultures (31). Involvement of

miR-449 family members in vertebrate multiciliogenesis has been previously reported (29). From these data, it can be suggested that these miRNAs might be playing an active role in the regulation of epithelial cell differentiation. Two wellknown miRNA clusters were found to be down-regulated in NHBE differentiated cells: clusters 17–92 and 106–363. Members of these clusters are considered as oncomirs, but, at the same time, cluster 17–92 has been associated with differentiation of macrophages, T cells, and spermatogonia (32–34). Moreover, transgenic overexpression of cluster 17–92 promotes proliferation and inhibits differentiation of lung epithelial progenitor cells (35), directly linking these cluster members to airway epithelial differentiation. In this sense, the global miRNA expression profile found in our model seems to be in agreement with previous studies.

Gene array analysis generated a large list of genes showing significant changes during the differentiation process of NHBE cells, many of which have established functions in the respiratory epithelium. Among them, there are genes encoding cytokines, secreted proteins, cell surface and adhesion molecules, cytoskeleton proteins, transcription factors, genes involved in cellular metabolism, and cell cycle and apoptosis. Secretoglobins, major histocompatibility complex molecules, mucins and dyneins, tubulins, and keratins are some of the genes presenting the greatest changes between undifferentiated and differentiated NHBE cells. In a previous report by Ross and coworkers (36), similar subsets of genes were found increased in differentiated compared with undifferentiated bronchial epithelial cells. An enrichment analysis of differentially expressed genes showed a predominance of categories related to structural changes linked to differentiation, such as cilium biogenesis and extracellular matrix components in the clusters comprising genes up-regulated in differentiated compared with undifferentiated cells. The clusters including genes down-regulated in differentiated compared with undifferentiated cells were enriched in biological categories mainly related to cell cycle progress and regulation, in accordance with the higher proliferative state of undifferentiated cells.

We were interested in miRNAs that regulate genes related to proliferation and differentiation processes of airway epithelium. Once we selected the miRNAs presenting the most pronounced changes between undifferentiated and differentiated cells, computational tools were used to identify potential targets. We focused on the list of putative targets that might be involved in the proliferation of basal cells or markers of differentiated cells (ciliated and mucus-secreting cells). CDC25A is a cell cycle phosphatase required for the regulation of both G1/S and G2/M phase transition during cell cycle progression (37). Although several papers deal with the regulation of CDC25A by different miRNAs in relation to cancer progression (38–40), only one reports a physiologic role for miRNA (miR-322/424 and miR-503) in regulating CDC25A during the differentiation of myoblasts into myotubes in muscle (41). In the present study, and in keeping with previous studies dealing with the differentiation process of bronchial and nasal epithelial cells (29, 36), CDC25A expression was found to be down-regulated in differentiated compared with undifferentiated NHBE cells. This result is in accordance with the function of CDC25A, as undifferentiated cells are in a high proliferative state (high levels of CDC25A), whereas differentiated cells show minimal proliferation (low levels of CDC25A). In contrast, miR-449a was found to be up-regulated in differentiated compared with undifferentiated cells, showing the expected inverse expression relationship between a miRNA and its putative target. Moreover, the regulatory effect of miR-449a on CDC25A has been recently reported in different cellular models, such as human nasal epithelial cells, human embryonic kidney 293 cells, bladder cancer cells, and the osteosarcoma cell line, saos-2 (29, 39, 40). For this reason, miR-449a and CDC25A were selected for further study in our physiological model of epithelial differentiation. We used a lentiviral vector expressing an anti-miR to miR-449a to block it in NHBE cells, which leads to an increase in CDC25A protein expression. Due to the low CDC25A protein expression levels in fully differentiated cells (Day 28 of ALI culture), the transduction experiments in NHBE cells with lentiviral particles were performed at Day 14 of ALI culture, when cells are already partially differentiated. Although there might be differences in the expression levels of MUC1, CDC25A, miR-449a, and miR-455-3p between Days 14 and 28 of ALI culture, the expression of these genes and miRs at Day 14 (differentiation in progress) was changing in a similar manner to the expression levels observed at Day 28 of ALI (final differentiation). Differentiated NHBE cells are difficult to transfect; therefore, we used A549 cells for the luciferase reporter experiments. A549 cells represent a lung epithelial cell convenient for our study, because they express both CDC25A and MUC1. In this way, miR-449a seems to be targeting and decreasing CDC25A protein expression by directly binding to its 3'-UTR in A549 cells. This direct relationship has been previously reported in human embryonic kidney 293T cells (29). Therefore, our findings support the role of miR-449a in the differentiation of NHBE cells via regulation of the expression of CDC25A at the translational level, possibly by binding to CDC25A 3'-UTR.

MUC1 is a membrane-bound glycoprotein that is expressed in most epithelial cells and aberrantly overexpressed in various carcinomas and inflammatory diseases (42). In physiological conditions, MUC1, together with other mucins, plays an important role in protecting normal cells from pathogens. In our model of airway epithelial differentiation, MUC1 expression was greatly increased in differentiated compared with undifferentiated cells, a result that is consistent with previous findings (36). MUC5AC and MUC5B mucins are known to be highly expressed in differentiated NHBE cells. However, no miRNA seemed to have MUC5AC as a putative target. In addition, miR-125b was the only miR in our list potentially targeting MUC5B, but the changes

found over differentiation for this miR were much smaller than the ones for miR-455-3p, a miR potentially regulating MUC1. For this reason, we selected MUC1 as an NHBE cell differentiation marker and the decreased miR-455-3p as its potential regulator. After overexpressing miR-455-3p in NHBE cells through transduction of lentiviral particles containing a miR-455-3p precursor, MUC1 mRNA and protein expression levels were found significantly decreased. Moreover, miR-455-3p-mediated suppression of MUC1 seemed to be dependent on the MUC1 3'-UTR. Therefore, these results highlight the importance of miR-455-3p as a regulator of the differentiation process of airway epithelium by targeting MUC1 at both post-transcriptional and translational levels. To date, three miRNAs (miR-125b, miR-145, and miR-1226) have been reported to regulate the expression of MUC1 in different breast cancer cell lines, emphasizing the role of MUC1 as an oncoprotein (43–45). In the present study, we demonstrated a physiological role of miR-455-3p regulating MUC1 expression in NHBE cells.

Collectively, our study provides novel data on the miRNA profile of NHBE cells in undifferentiated and differentiated states, and demonstrates for the first time, the direct regulation exerted by miR-455-3p on MUC1 in our bronchial epithelium model. It also confirms the regulatory relationship between miR-449a and CDC25A in differentiated NHBE cells. Both, MUC1 and CDC25A, together with miR-455-3p and miR-449a, can serve as biomarkers for the differentiation of bronchial epithelia.

Author disclosures are available with the text of this article at www.atsjournals.org.

Acknowledgments: The authors thank the Biological Imaging Section/Research Technology Branch at the National Institute of Allergy and Infectious Diseases (National Institutes of Health) for their contribution in confocal imaging and image post-processing.

References

- Harkema JR, Mariassy A, St. George J, Hyde DM, Plopper CG. Epithelial cells of the conducting airways: a species comparison. In: Farmer SG, Hay DWP, eds. *The airway epithelium: physiology, pathophysiology and pharmacology*. New York: Marcel-Dekker Press; 1991. pp. 3–39.
- Cohen TS, Prince A. Cystic fibrosis: a mucosal immunodeficiency syndrome. *Nat Med* 2012;18:509–519.
- Holgate ST. The sentinel role of the airway epithelium in asthma pathogenesis. *Immunol Rev* 2011;242:205–219.
- Spurzem JR, Rennard SI. Pathogenesis of COPD. *Semin Respir Crit Care Med* 2005;26:142–153.
- Gray TE, Guzman K, Davis CW, Abdullah LH, Nettesheim P. Mucociliary differentiation of serially passaged normal human tracheobronchial epithelial cells. *Am J Respir Cell Mol Biol* 1996;14:104–112.
- Dvorak A, Tilley AE, Shaykhiyev R, Wang R, Crystal RG. Do airway epithelium air-liquid cultures represent the *in vivo* airway epithelium transcriptome? *Am J Respir Cell Mol Biol* 2011;44:465–473.
- Pezzulo AA, Starner TD, Scheetz TE, Traver GL, Tilley AE, Harvey BG, Crystal RG, McCray PB Jr, Zabner J. The air-liquid interface and use of primary cell cultures are important to recapitulate the transcriptional profile of *in vivo* airway epithelia. *Am J Physiol Lung Cell Mol Physiol* 2011;300:L25–L31.
- Kesimer M, Kirkham S, Pickles RJ, Henderson AG, Alexis NE, Demaria G, Knight D, Thornton DJ, Sheehan JK. Tracheobronchial air-liquid interface cell culture: a model for innate mucosal defense of the upper airways? *Am J Physiol Lung Cell Mol Physiol* 2009;296:L92–L100.
- LeSimple P, Liao J, Robert R, Gruenert DC, Hanrahan JW. Cystic fibrosis transmembrane conductance regulator trafficking modulates the barrier function of airway epithelial cell monolayers. *J Physiol* 2010;588:1195–1209.
- Lopez-Souza N, Favoreto S, Wong H, Ward T, Yagi S, Schnurr D, Finkbeiner WE, Dolganov GM, Widdicombe JH, Boushey HA, et al. *In vitro* susceptibility to rhinovirus infection is greater for bronchial than for nasal airway epithelial cells in human subjects. *J Allergy Clin Immunol* 2009;123:1384–1390, e2.

11. John G, Yildirim AO, Rubin BK, Gruenert DC, Henke MO. TLR-4-mediated innate immunity is reduced in cystic fibrosis airway cells. *Am J Respir Cell Mol Biol* 2010;42:424–431.
12. Hackett TL, Warner SM, Stefanowicz D, Shaheen F, Pechkovsky DV, Murray LA, Argentieri R, Kicic A, Stick SM, Bai TR, *et al.* Induction of epithelial-mesenchymal transition in primary airway epithelial cells from patients with asthma by transforming growth factor- β 1. *Am J Respir Crit Care Med* 2009;180:122–133.
13. Thompson HG, Mih JD, Krasieva TB, Tromberg BJ, George SC. Epithelial-derived TGF- β 2 modulates basal and wound-healing subepithelial matrix homeostasis. *Am J Physiol Lung Cell Mol Physiol* 2006;291:L1277–L1285.
14. Casalino-Matsuda SM, Monzón ME, Forteza RM. Epidermal growth factor receptor activation by epidermal growth factor mediates oxidant-induced goblet cell metaplasia in human airway epithelium. *Am J Respir Cell Mol Biol* 2006;34:581–591.
15. He L, Hannon GJ. MicroRNAs: small RNAs with a big role in gene regulation. *Nat Rev Genet* 2004;5:522–531.
16. Filipowicz W, Bhattacharyya SN, Sonenberg N. Mechanisms of post-transcriptional regulation by microRNAs: are the answers in sight? *Nat Rev Genet* 2008;9:102–114.
17. Karp X, Ambros V. Developmental biology: encountering microRNAs in cell fate signaling. *Science* 2005;310:1288–1289.
18. Bueno MJ, Pérez de Castro I, Malumbres M. Control of cell proliferation pathways by microRNAs. *Cell Cycle* 2008;7:3143–3148.
19. Chen CZ, Li L, Lodish HF, Bartel DP. MicroRNAs modulate hematopoietic lineage differentiation. *Science* 2004;303:83–86.
20. Xu P, Guo M, Hay BA. MicroRNAs and the regulation of cell death. *Trends Genet* 2004;20:617–624.
21. Liston A, Linterman M, Lu LF. MicroRNA in the adaptive immune system, in sickness and in health. *J Clin Immunol* 2010;30:339–346.
22. Esau C, Kang X, Peralta E, Hanson E, Marcussen EG, Ravichandran LV, Sun Y, Koo S, Perera RJ, Jain R, *et al.* MicroRNA-143 regulates adipocyte differentiation. *J Biol Chem* 2004;279:52361–52365.
23. Zhao Y, Samal E, Srivastava D. Serum response factor regulates a muscle-specific microRNA that targets Hand2 during cardiogenesis. *Nature* 2005;436:214–220.
24. Kuwabara T, Hsieh J, Nakashima K, Taira K, Gage FH. A small modulatory dsRNA specifies the fate of adult neural stem cells. *Cell* 2004;116:779–793.
25. Tsuchiya S, Oku M, Imanaka Y, Kunimoto R, Okuno Y, Terasawa K, Sato F, Tsujimoto G, Shimizu K. MicroRNA-338-3p and microRNA-451 contribute to the formation of basolateral polarity in epithelial cells. *Nucleic Acids Res* 2009;37:3821–3827.
26. Carraro G, El-Hashash A, Guidolin D, Tiozzo C, Turcatel G, Young BM, De Langhe SP, Bellusci S, Shi W, Parnigotto PP, *et al.* miR-17 family of microRNAs controls FGF10-mediated embryonic lung epithelial branching morphogenesis through MAPK14 and STAT3 regulation of E-cadherin distribution. *Dev Biol* 2009;333:238–250.
27. Nguyen HT, Dalmasso G, Yan Y, Laroui H, Dahan S, Mayer L, Sitaraman SV, Merlin D. MicroRNA-7 modulates CD98 expression during intestinal epithelial cell differentiation. *J Biol Chem* 2010;285:1479–1489.
28. Lu M, Shi B, Wang J, Cao Q, Cui Q. TAM: a method for enrichment and depletion analysis of a microRNA category in a list of microRNAs. *BMC Bioinformatics* 2010;11:419.
29. Marcet B, Chevalier B, Luxardi G, Coraux C, Zaragosi LE, Cibois M, Robbe-Sermesant K, Jolly T, Cardinaud B, Moreilhon C, *et al.* Control of vertebrate multiciliogenesis by miR-449 through direct repression of the Delta/Notch pathway. *Nat Cell Biol* 2011;13:693–699.
30. Aranha MM, Santos DM, Solá S, Steer CJ, Rodrigues CM. miR-34a regulates mouse neural stem cell differentiation. *PLoS ONE* 2011;6:e21396.
31. Ramachandran S, Karp PH, Jiang P, Ostedgaard LS, Walz AE, Fisher JT, Keshavjee S, Lennox KA, Jacobi AM, Rose SD, *et al.* A microRNA network regulates expression and biosynthesis of wild-type and DeltaF508 mutant cystic fibrosis transmembrane conductance regulator. *Proc Natl Acad Sci USA* 2012;109:13362–13367.
32. Tong MH, Mitchell DA, McGowan SD, Evanoff R, Griswold MD. Two miRNA clusters, Mir-17-92 (Mirc1) and Mir-106b-25 (Mirc3), are involved in the regulation of spermatogonial differentiation in mice. *Biol Reprod* 2012;86:72.
33. Jiang S, Li C, Olive V, Lykken E, Feng F, Sevilla J, Wan Y, He L, Li QJ. Molecular dissection of the miR-17-92 cluster's critical dual roles in promoting Th1 responses and preventing inducible Treg differentiation. *Blood* 2011;118:5487–5497.
34. Pospisil V, Vargova K, Kokavec J, Rybarova J, Savvulidi F, Jonasova A, Necas E, Zavadil J, Laslo P, Stopka T. Epigenetic silencing of the oncogenic miR-17-92 cluster during PU.1-directed macrophage differentiation. *EMBO J* 2011;30:4450–4464.
35. Lu Y, Thomson JM, Wong HY, Hammond SM, Hogan BL. Transgenic over-expression of the microRNA miR-17-92 cluster promotes proliferation and inhibits differentiation of lung epithelial progenitor cells. *Dev Biol* 2007;310:442–453.
36. Ross AJ, Dailey LA, Brighton LE, Devlin RB. Transcriptional profiling of mucociliary differentiation in human airway epithelial cells. *Am J Respir Cell Mol Biol* 2007;37:169–185.
37. Ray D, Kiyokawa H. CDC25A levels determine the balance of proliferation and checkpoint response. *Cell Cycle* 2007;6:3039–3042.
38. Wang P, Zou F, Zhang X, Li H, Dulak A, Tomko RJ Jr, Lazo JS, Wang Z, Zhang L, Yu J. microRNA-21 negatively regulates Cdc25A and cell cycle progression in colon cancer cells. *Cancer Res* 2009;69:8157–8165.
39. Yang X, Feng M, Jiang X, Wu Z, Li Z, Aau M, Yu Q. miR-449a and miR-449b are direct transcriptional targets of E2F1 and negatively regulate pRb-E2F1 activity through a feedback loop by targeting CDK6 and CDC25A. *Genes Dev* 2009;23:2388–2393.
40. Chen H, Lin YW, Mao YQ, Wu J, Liu YF, Zheng XY, Xie LP. MicroRNA-449a acts as a tumor suppressor in human bladder cancer through the regulation of pocket proteins. *Cancer Lett* 2012;320:40–47.
41. Sarkar S, Dey BK, Dutta A. MiR-322/424 and -503 are induced during muscle differentiation and promote cell cycle quiescence and differentiation by down-regulation of CDC25A. *Mol Biol Cell* 2010;21:2138–2149.
42. Bafna S, Kaur S, Batra SK. Membrane-bound mucins: the mechanistic basis for alterations in the growth and survival of cancer cells. *Oncogene* 2010;29:2893–2904.
43. Jin C, Rajabi H, Kufe D. miR-1226 targets expression of the mucin 1 oncoprotein and induces cell death. *Int J Oncol* 2010;37:61–69.
44. Rajabi H, Jin C, Ahmad R, McClary C, Joshi MD, Kufe D. Mucin 1 oncoprotein expression is suppressed by the miR-125b oncomir. *Genes Cancer* 2010;1:62–68.
45. Sachdeva M, Mo YY. MicroRNA-145 suppresses cell invasion and metastasis by directly targeting mucin 1. *Cancer Res* 2010;70:378–387.